IEEE Photonics Journal
An IEEE Photonics Society Publication

Open Access

An Ultracompact Multimode Waveguide Crossing Based on Subwavelength Asymmetric Y-Junction

Volume 10, Number 4, August 2018

Weijie Chang
Luluzi Lu
Xinshu Ren
Longhui Lu
Mengfan Cheng
Deming Liu
Minming Zhang

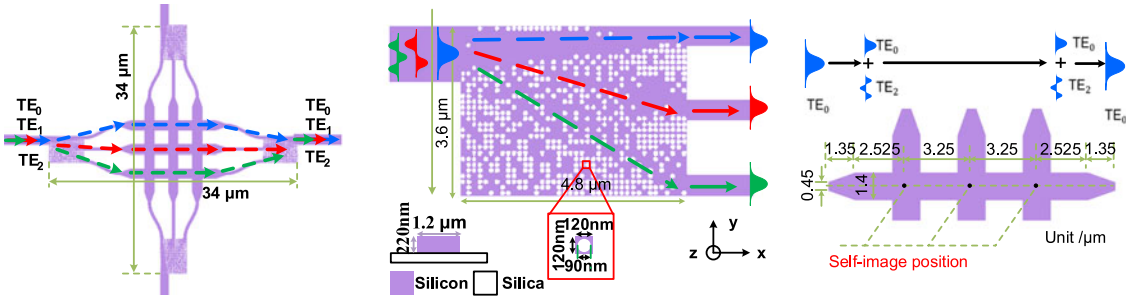

(a) (b) (c)

DOI: 10.1109/JPHOT.2018.2847762
1943-0655 © 2018 IEEE

An Ultracompact Multimode Waveguide Crossing Based on Subwavelength Asymmetric Y-Junction

Weijie Chang, Luluzi Lu, Xinshu Ren, Longhui Lu, Mengfan Cheng, Deming Liu, and Minming Zhang

School of Optical and Electronic Information, Huazhong University of Science and Technology, Wuhan 430074, China

DOI:10.1109/JPHOT.2018.2847762

Manuscript received May 10, 2018; revised June 10, 2018; accepted June 12, 2018. Date of publication June 15, 2018; date of current version June 22, 2018. This work was supported in part by the National Natural Science Foundation of China under Grant 61775069 and in part by the Fundamental Research Funds for the Central Universities, Huazhong University of Science and Technology under Grant 2017KFXKJC002. Corresponding author: Minming Zhang (e-mail: mmz@mail.hust.edu.cn).

Abstract: We propose and experimentally demonstrate a novel ultracompact multimode waveguide crossing. The compact asymmetric subwavelength Y-junction is introduced to convert the high-order modes into fundamental ones, enabling one to implement three or more modes simultaneously in the subsequent processing. Our proposed device occupied only a compact footprint of 34 $\times$ 34 μm^2. The measured results indicate our fabricated device exhibited a high performance with the insertion loss less than 0.9 dB, crosstalk lower than –24 dB from 1.52 to 1.60 μm for all the three modes. Moreover, our scheme could be easily expended to implement more modes and will show great potential in dense and large-scale on-chip photonic integration.

Index Terms: Integrated optics devices, mode-division multiplexing, metamaterials.

1. Introduction

Recently, mode-division multiplexing (MDM) on silicon-on-insulator (SOI) platform, as a more promising and attractive technology, provides an effective approach to further increase the transmission capacity of on-chip optical interconnect [1]. To realize MDM communication system, various key building blocks have been extensively demonstrated, typically including mode (de) multiplexers ((DE) MUX) [2]–[6], multimode bent waveguides [7]–[9] and mode switch [10]–[12]. A compact multimode waveguide crossing, as an essential component for realizing a densely integrated MDM optical interconnect network, has been rarely addressed due to the complex mode coupling at the crossing region for high order modes. Recently, self-image effect in the conventional multimode-interference (MMI) couplers has been utilized to realize the dual mode waveguide crossing [13]. Unfortunately, the severe self-image positions offset between the fundamental mode and first-order mode in conventional waveguide leads to a relatively large coupling length and complicate design process. Therefore, one may use symmetric Y-junction to convert both fundamental mode and first-order mode to two in-phase or anti-phase single mode parts for mode crossing interconnect via a 2 $\times$ 2 single mode waveguide crossing array [14]. It works very well for two modes. However, due to severe modal mismatch in symmetric Y-junction, the scheme may be not suitable for implementing

more modes, which might limit its potential application in large-scale MDM system. A compact multimode waveguide crossing for implementing three or more modes simultaneously is still an urgent issue for dense and large-scale MDM photonic integration.

To implement three or more modes simultaneously, converting high order modes to the individually fundamental modes provides an effective approach in the multimode communication applications. Multimode waveguide crossing can be also designed in this way. However, a multimode convertor based on the conventional waveguide such as asymmetric directional coupler or asymmetric Y-junction usually suffers from a quite large scale (hundreds of microns) [15], [16]. As the mode channels increase, the footprint of these structure will increase dramatically, which apparently prevents its practical application for dense and large-scale MDM photonic integration. As a result, an ultra-compact multimode convertor, as an essential component, plays a dominant role in such design process. Recently, enabling one to manipulate light field and engineer the refractive index distribution at the subwavelength scale, free-form or digital silicon subwavelength (SW) structures offer a promising platform to realize ultra-compact and highly functional devices simultaneously [17]–[21]. Furthermore, to suppress the main fabrication errors caused by the lag effect in the plasma etching process, we have proposed a fabrication-error-insensitive PhC-like SW structure [22]. Various optimization algorithms including particle swarm, topological optimization, genetic algorithm and direct binary search (DBS) have been proposed for inverse design. Compared with other optimization algorithms, DBS algorithm is more suitable and effective for optimizing discretized binary units. Recently, an ultra-compact and high performance asymmetric Y-junction based on PhC-like SW structure using DBS method has been proposed and experimentally demonstrated to convert high order modes to the individually corresponding fundamental modes in our previous work [23].

In this paper, we propose a novel ultra-compact multimode waveguide crossing which could implement three or more modes simultaneously. The proposed device is composed of four asymmetric Y-junctions and a N $\times$ N single mode waveguide crossing array. The asymmetric Y-junction based on subwavelength (SW) structure is introduced to convert all the input N-order transverse electric (TE_n) eigenmodes to N local fundamental modes to ease the subsequent processing, respectively. Moreover, it occupies an ultra-compact footprint of only several μm^2. The N $\times$ N single mode waveguide crossing array could be achieved by the cascaded multimode-interference couplers in only a compact footprint [24]. In our work, the three-mode waveguide crossing is utilized as a representative for example. Here, we have designed, characterized and experimentally demonstrated a multimode waveguide crossing. The fabricated device occupied a compact footprint of only 34 $\times$ 34 μm^2, which is the most compact footprint that have been reported to the best of our knowledge, and exhibited high performance with insertion losses (ILs) lower than 2 dB and crosstalks (CTs) less than -20 dB for all the modes over a wavelength range of 60 nm centered at 1560 nm.

2. Operation Principle

Figure 1(a) shows the operation principle for the multimode waveguide crossing. The proposed structure is composed of four SW structure asymmetric Y-junctions and a 3 $\times$ 3 single mode waveguide crossing array based on MMI couplers. The proposed device is designed on a SOI platform with 220 nm-thick silica-cladded top silicon layer. The asymmetric Y-junction based on PhC-like SW structure is designed and optimized using the inverse design method, as shown in Fig. 1(b) [23]. It takes 192 hours to get the optimized nanopattern after 4 rounds of iteration on a computer with an 8-core central processing unit (Intel Xeon E5-2637). The asymmetric Y-junction works as a mode convertor to make the TE_n modes evolve into the corresponding fundamental modes, which could release the subsequent processing greatly. Therefore, the subsequent 3 $\times$ 3 crossing array only needs to be optimized and designed for the single mode. For a clear illustration, part of the optimized crossing array is illustrated in Fig. 1(c). Due to the axisymmetric structure, the injected TE_0 could only excite TE_0 and TE_2, while the injected TE_1 could only excite TE_1 and TE_3 similarly. According to the self-image effect of multimode interference, the N fold images of the TE_0 could be periodically formed at the center of the waveguide crossings [24], [25]. At the output

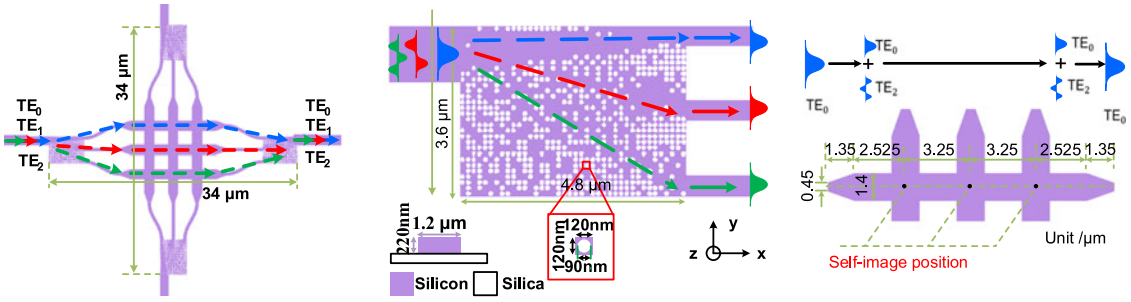

(a) (b) (c)

Fig. 1. (a) Schematic structure for multimode waveguide crossing. (b) Asymmetric Y-junction (c) Part of 3 × 3 waveguide crossing array for the single mode.

port, a mirrored asymmetric Y-junction is also employed to reconvert the fundamental modes to corresponding TE_n modes. In this way, a three-mode waveguide crossing is designed. Furthermore, our scheme could be also extended to implement more modes.

The proposed device is designed on a SOI platform with 220 nm-thick silica-cladded top silicon layer. The SW structure asymmetric Y-junction based on PhC-like SW consists of 30 × 40 pixels. Each pixel is in the shape of a silicon square (120 × 120 nm^2) with a central circular hole (radius r = 45 nm, etch depth = 220 nm). By engineering the metamaterial refractive index between the three arms and manipulating the phase profile of optical field at the nanoscale, a wide-angle asymmetric Y-junction is achieved and the footprint of the device can be dramatically reduced. As shown in Fig. 1(b), the device occupies the compact footprint of only 3.6 × 4.8 μm^2. The gaps between the branches of asymmetric Y-junctions are 1.575 μm. Single mode waveguides with the length of 5 μm are used to connect asymmetric Y-junction and the 3 × 3 waveguide crossing array. For the 3 × 3 waveguide crossing array, the nonadiabatic taper is adopted with a width range linearly varying from 0.45 μm to 1.4 μm within a length of 1.35 μm to connect single mode waveguide. The coupling length from the taper to the center of the left waveguide crossing intersection is 2.525 μm, and the distance between the two centers of the adjacent waveguide intersection is 3.25 μm. Thus, our proposed multimode waveguide crossing occupies a compact footprint of only 34 × 34 μm^2, which may be the most compact footprint that have been reported to the best of our knowledge.

3D finite-difference time-domain (FDTD) simulation via a commercial software (Lumerical FDTD Solutions) is utilized to evaluate the performance of the proposed multimode waveguide based on the SW structure asymmetric Y-junction [26]. The magnetic field distributions at 1560 nm wavelength for TE_0, TE_1 and TE_2 are illustrated in Figs. 2(a)–2(c), respectively. As expected, the SW structure asymmetric Y-junction converts the TE_n modes to the corresponding local fundamental modes to relax the subsequent processing, and the mirrored SW structure asymmetric Y-junction reconverts the fundamental modes to corresponding TE_n modes at the output port. The simulated transmission spectra for TE_0, TE_1 and TE_2 injected in the input waveguide are presented in Figs. 2(d)–2(f), respectively. Here, the IL_n and CT_n for TE_n are defined as:

$$IL_n = -10 \cdot \log(T_n) \tag{1}$$

$$CT_n = 10 \cdot \log_{10}\left(\frac{\max\{T_{j(j\neq n)}\}}{T_n}\right) \tag{2}$$

where T_j and T_n denote the transmittance for TE_j and TE_n mode at the output ports, respectively. The simulated ILs for TE_0, TE_1 and TE_2 are less than 1.5 dB and the CTs for all the modes are lower than –22 dB over a wavelength range from 1520 to 1580 nm, respectively.

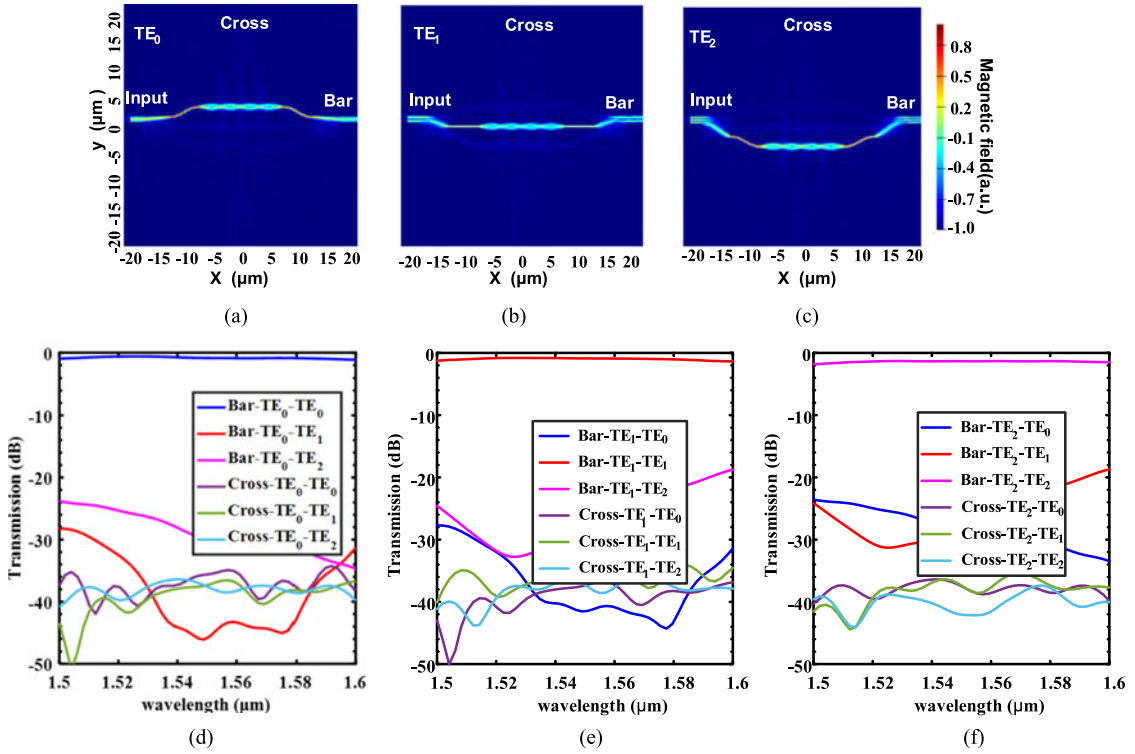

Fig. 2. (a)–(c) Simulated magnetic field distributions for TE_0, TE_1 and TE_2, respectively. (c)–(d) Simulated transmission spectra for TE_0, TE_1 and TE_2 injected in the input waveguide, respectively.

3. Experiment Results

The proposed ultra-compact multimode waveguide crossing based on a SW structure asymmetric Y-junction was fabricated and experimentally demonstrated. The electron-beam lithography (EBL) system (Vistec EBPG 5000 Plus) was used to form the designed pattern on a SOI platform with a 220 nm-thick top silicon layer, and the inductively coupled plasma (ICP) etcher (Plasmalab System100) was utilized to transfer the mask to the silicon device layer. Finally, the fabricated device is covered by the 1.2 μm-thick SiO_2 cladding. Despite of the lag effect, the nanoholes could be actually ensured to be fully etched by increasing the etching time [23]. The SW structure asymmetrical Y-junction based MUX was utilized to excite the higher order modes [23]. Besides, an extra reference MDM system was also fabricated to evaluate the performance of the device.

The top-view scanning electron microscope (SEM) pictures of the reference MDM system and the detailed DEMUX are illustrated in Figs. 3(a) and 3(b). A broad amplified spontaneous emission (ASE) light source and an optical spectrum analyzer (Yokogawa AQ6370C–20) were utilized to measure the spectral transmission over a wide wavelength range from 1.52 to 1.6 μm. The grating couples for TE polarization were used in our experimental measurement. Figs. 3(c)–3(e) show the measured spectral transmission for the reference MDM system when the light was launched in I1 (TE_0 mode), I2 (TE_1 mode) and I3 (TE_2 mode). The measured average ILs for TE_0, TE_1 and TE_2 were less than 1.6 dB and the measured CTs for all the modes were lower than –22 dB over an operating width of 60 nm centered at 1560 nm, respectively.

Figure 4(a) shows the top-view SEM image of the fabricated device composed of a multimode waveguide crossing, a MUX and a DEMUX. The detailed SEM images of the fabricated SW structure asymmetric Y-junction, and DEMUX are illustrated in. Figs. 4(b)–4(c), respectively. From the spectral transmission scans for each combination of the input and output ports, the performance of the multimode waveguide crossing was characterized and illustrated in Fig. 4(d)–4(f). “1-2” denotes the

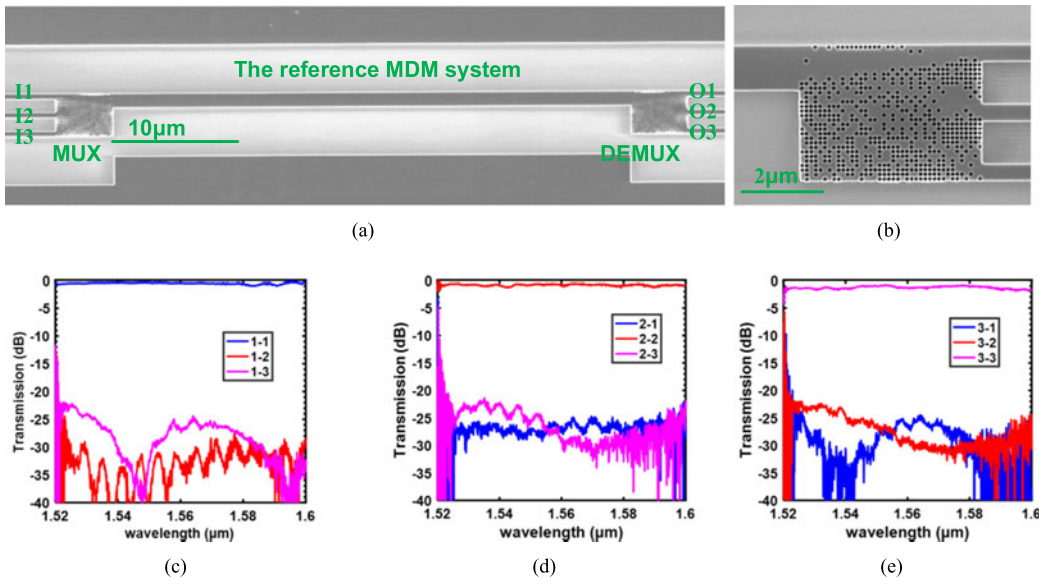

Fig. 3. (a) SEM image for the fabricated reference MDM system. (b) The detailed SEM picture for the DEMUX. (c)–(e) The measured transmission spectra for TE_0 injected in the upper, middle, lower input waveguides, respectively.

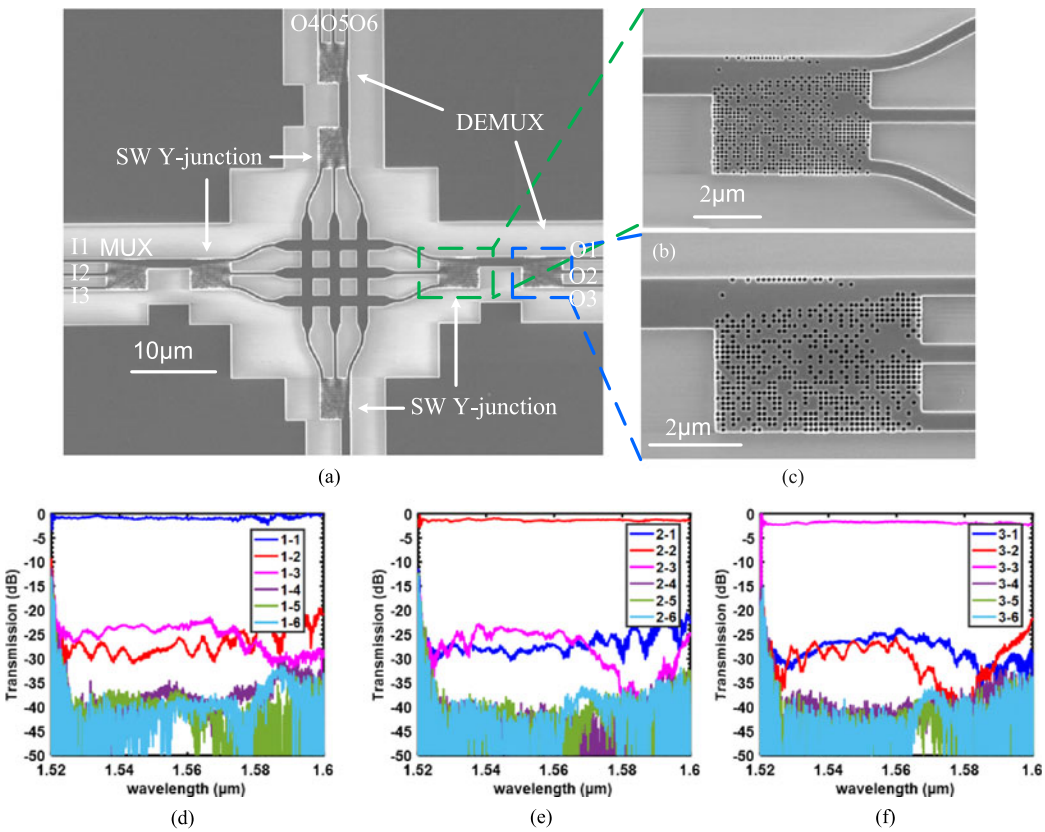

Fig. 4. (a) SEM image for the fabricated reference MDM system. (b) The detailed SEM picture for the DEMUX. (d)–(f) The measured transmission spectra for TE_0 injected in the upper, middle, lower input waveguides, respectively.

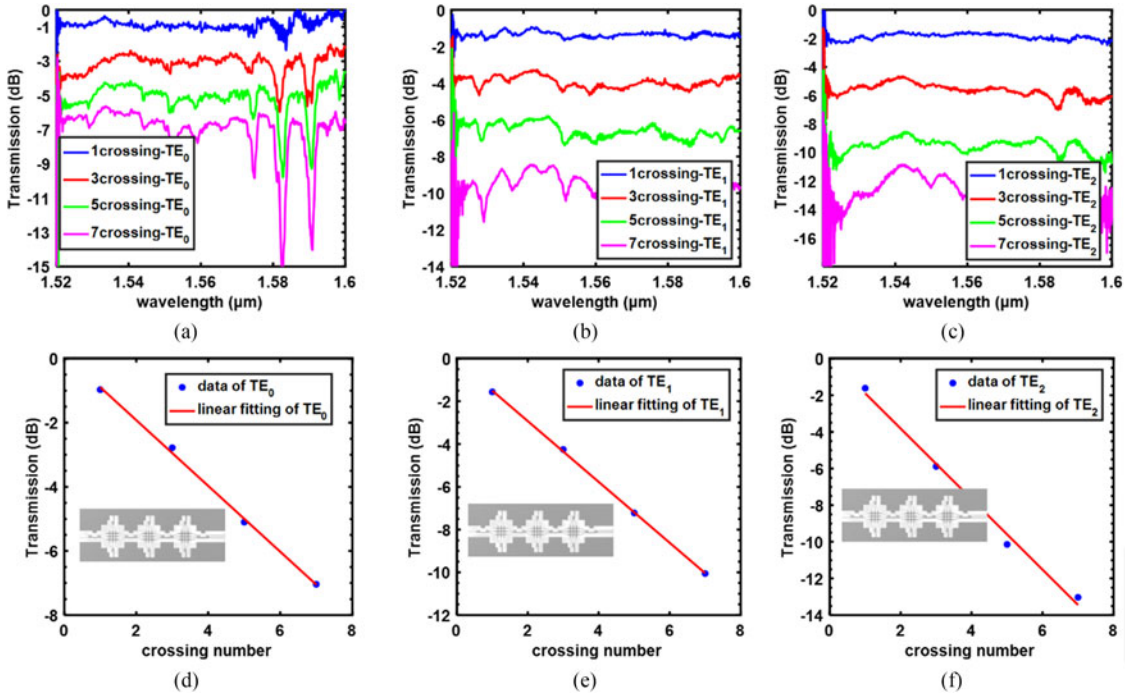

Fig. 5. (a)–(c) Measured normalized transmission spectra with different numbers of cascaded crossings for TE_0, TE_1, and TE_2, respectively. (d)–(f) The measured ILs at 1560 nm as a function of cased crossing numbers for TE_0, TE_1, and TE_2, respectively.

spectral transmission from input port 1 (I1) to output port 2 (O2). TE_0, TE_1 and TE_1 were excited when the light was launched in input port I1, I2 and I3, respectively. The measured normalized average ILs were less than 2 dB for all the modes from 1530 nm to 1590 nm. The measured CTs at the bar port and the cross port were less than $-$;20 dB and $-$;35 dB from 1530 nm to 1590 nm, respectively. To the best of our knowledge, our fabricated multimode crossing only occupied a footprint of 34 $\times$ 34 μm^2, which is the most compact scale that has been reported.

To further verify the ILs for all the modes and minimize the measurement errors, we also designed, fabricated and experimentally characterized three, five and seven cascaded crossings. The measured ILs for TE_0, TE_1 and TE_2 modes are illustrated in Figs. 5(a)–5(c). Due to the reflection between the mirrored asymmetric Y-junctions of the multimode waveguide crossing in the periodical cascaded structure, the Fabry–Perot resonances was observed in the fabricated devices. The length of cavity of periodical cascaded structure is 34 μm. The interval between the neighboring Fabry–Perot resonances around 1550 nm is approximately 9 nm, as given in Fig. 5(a). The intervals are theoretically calculated to be 8.86 nm according to the Fabry–Perot cavity length of 34 μm, which has a well agreement with our measured one. Figs. 5(d)–5(f) show the normalized transmittance as a function of the cascaded crossings number for TE_0, TE_1 and TE_2 at 1560 nm, respectively. The average ILs for TE_0, TE_1 and TE_2 obtained from the slop of linear fitting plots are 1 dB, 1.42 dB and 1.92 per crossing at 1560 nm. Meanwhile, the measured average ILs for all the modes were less than 2 dB over an operating bandwidth of 60 nm centered at 1560 nm. We believe the proposed device would show great potential in densely integrated multi-mode transmission system for on-chip optical interconnect.

We also investigate the fabrication tolerance of the SW structure asymmetric Y-junction, since it accounts for the dominant ILs for our proposed device. The average transmission spectra of TE_0, TE_1 and TE_2 for the SW structure asymmetric Y-junction as a function of various holes' radii from 40 to 50 nm are illustrated in Figs. 6(e)–6(f), respectively. The simulation results demonstrate ILs

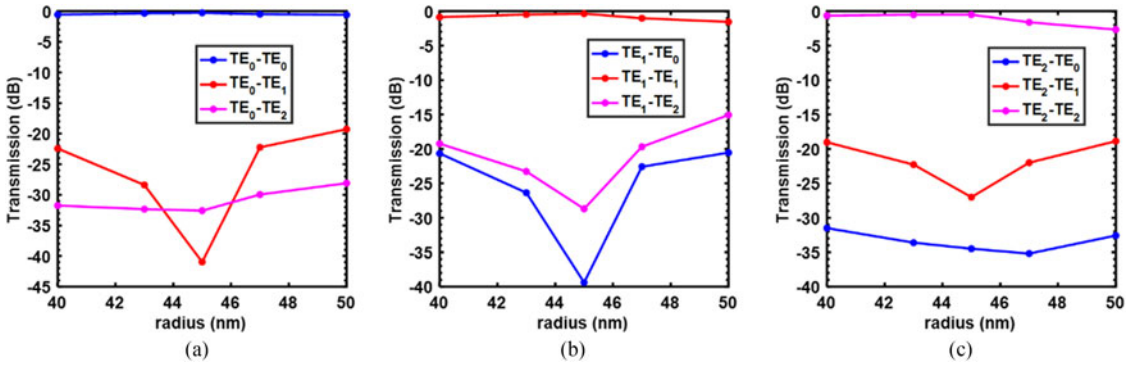

Fig. 6. (a)–(c) Simulated average transmission spectra of TE_0, TE_1 and TE_2 for the SW structure asymmetric Y-junction as a function of holes radii, respectively.

for all the modes increase about 1 dB in average and CTs are still less than -18 dB as the radius of nanoholes decrease by -5 nm compared with the optimized radius of 45 nm. However, we also find that the asymmetric Y-junction exhibits a relatively severe deterioration when the holes' radius is larger than 45 nm, which probably occurs to an over etching device. To suppress the dominant fabrication errors for over etching, we may estimate the ICP etching velocity before etching the device and then set an appropriate corresponding etching time ($\sim$36 s). Therefore, the low ILs for our proposed device could be achieved in this way.

4. Conclusion

In summary, we have proposed and experimentally demonstrated an ultra-compact multimode waveguide crossing which could implement three modes simultaneously. The SW structure asymmetric Y-junction is introduced to convert all the N-order eiginmodes to the N local fundamental modes to ease the subsequent processing. The footprint of the fabricated ultra-compact multimode waveguide crossing was 34 $\times$ 34 μm^2. The measured results exhibited a high performance with the average ILs lower than 2 dB and the CTs less than -20 dB for all the modes over an operating bandwidth of 60 nm centered at 1560 nm. Our proposed scheme could be easily expended to implement more modes. We believe the proposed device would show great potential to promote practical applications of densely integrated photonic MDM systems for on-chip optical interconnect. Furthermore, the method of converting higher order modes to the fundamental mode may offer an attractive approach to implement on-chip multimode signal processing simultaneously.

References

[1] D. Dai and J. E. Bowers, "Silicon-based on-chip multiplexing technologies and devices for Peta-bit optical interconnects," *Nanophotonics*, vol. 3, no. 4, pp. 283–311, 2014.
[2] Y. Ding, J. Xu, F. Da Ros, B. Huang, H. Ou, and C. Peucheret, "On-chip two-mode division multiplexing using tapered directional coupler-based mode multiplexer and demultiplexer," *Opt. Exp.*, vol. 21, no. 8, pp. 10376–10382, 2013.
[3] J. Wang, P. Chen, S. Chen, Y. Shi, and D. Dai, "Improved 8-channel silicon mode demultiplexer with grating polarizers," *Opt. Exp.*, vol. 22, no. 11, pp. 12799–12807, 2014.
[4] Z. Zhang, X. Hu, and J. Wang, "On-chip optical mode exchange using tapered directional coupler," *Sci. Rep.*, vol. 5, 2015, Art. no. 16072.
[5] T. Uematsu, Y. Ishizaka, Y. Kawaguchi, K. Saitoh, and M. Koshiba, "Design of a compact two-mode multi/demultiplexer consisting of multimode interference waveguides and a wavelength-insensitive phase shifter for mode-division multiplexing transmission," *J. Lightw. Technol.*, vol. 30, no. 15, pp. 2421–2426, Aug. 2012.
[6] M. Ye, Y. Yu, J. Zou, W. Yang, and X. Zhang, "On-chip multiplexing conversion between wavelength division multiplexing-polarization division multiplexing and wavelength division multiplexing-mode division multiplexing," *Opt. Lett.*, vol. 39, pp. 758–761, 2014.
[7] C. Sun, Y. Yu, G. Chen, and X. Zhang, "Ultra-compact bent multimode silicon waveguide with ultralow inter-mode crosstalk," *Opt. Lett.*, vol. 42, pp. 3004–3007, 2017.

[8] H. Xu and Y. Shi, "Ultra-sharp multi-mode waveguide bending assisted with metamaterial-based mode converters," *Laser Photon. Rev.*, vol. 12, 2018, Art. no. 1700240.
[9] W. Chang, L. Lu, D. Liu, and M. Zhang, "Ultra-compact silicon multi-mode waveguide bend based on subwavelength asymmetric Y-junction," in *Proc. Opt. Fiber Commun. Conf.*, 2018, Paper Tu3A.1.
[10] Y. Zhang, Y. He, Q. Zhu, C. Qiu, and Y. Su, "On-chip silicon photonic 2 x 2 mode- and polarization-selective switch with low inter-modal crosstalk," *Photon. Res.*, vol. 5, pp. 521–526, 2017.
[11] Y. Xiong, R. B. Priti, and O. Liboiron-Ladouceur, "High-speed two-mode switch for mode-division multiplexing optical networks," *Optica*, vol. 4, pp. 1098–1102, 2017.
[12] L. Yang *et al.*, "General architectures for on-chip optical space and mode switching," *Optica*, vol. 5, pp. 180–187, 2018.
[13] H. Xu and Y. Shi, "Dual-mode waveguide crossing utilizing taper-assisted multimode-interference couplers," *Opt. Lett.*, vol. 41, pp. 5381–5384, 2016.
[14] C. Sun, Y. Yu, and X. Zhang, "Ultra-compact waveguide crossing for a mode-division multiplexing optical network," *Opt. Lett.*, vol. 42, pp. 4913–4916, 2017.
[15] N. Riesen and J. D. Love, "Design of mode-sorting asymmetric Y-junctions," *Appl. Opt.*, vol. 51, no. 15, pp. 2778–2783, 2012.
[16] J. B. Driscoll, R. R. Grote, B. Souhan, J. I. Dadap, M. Lu, and R. M. Osgood, "Asymmetric Y junctions in silicon waveguides for on-chip mode-division multiplexing," *Opt. Lett.*, vol. 38, no. 11, pp. 1854–1856, 2013.
[17] A. Y. Piggott, J. Lu, K. G. Lagoudakis, J. Petykiewicz, T. M. Babinec, and J. Vučković, "Inverse design and demonstration of a compact and broadband on-chip wavelength demultiplexer," *Nature Photon.*, vol. 9, no. 6, pp. 374–377, 2015.
[18] B. Shen, P. Wang, R. Polson, and R. Menon, "An integrated-nanophotonics polarization beamsplitter with 2.4 $\times$ 2.4 μm^2 footprint," *Nature Photon.*, vol. 9, no. 6, pp. 378–382, 2015.
[19] A. Y. Piggott, J. Lu, T. M. Babinec, K. G. Lagoudakis, J. Petykiewicz, and J. Vučković, "Inverse design and implementation of a wavelength demultiplexing grating coupler," *Sci. Rep.*, vol. 4, no. 1, 2015, Art. no. 7210.
[20] Z. Yu, H. Cui, and X. Sun, "Genetic-algorithm-optimized wideband on-chip polarization rotator with an ultrasmall footprint," *Opt. Lett.*, vol. 42, no. 16, pp. 3093–3096, 2017.
[21] K. Xu *et al.*, "Integrated photonic power divider with arbitrary power ratios," *Opt. Lett.*, vol. 42, pp. 855–858, 2017.
[22] L. Lu *et al.*, "Inverse-designed single-stepetched colorless 3 dB couplers based on RIE-lag-insensitive PhC-like sub-wavelength structures," *Opt. Lett.*, vol. 41, no. 21, pp. 5051–5054, 2016.
[23] W. Chang *et al.*, "Ultra-compact mode (de) multiplexer based on subwavelength asymmetric Y-junction," *Opt. Exp.*, vol. 26, pp. 8162–8170, 2018.
[24] Y. Liu, J. M. Shainline, X. Zeng, and M. A. Popovic, "Ultra-low- loss CMOS-compatible waveguide crossing arrays based on multimode Bloch waves and imaginary coupling," *Opt. Lett.*, vol. 39, pp. 335–338, 2014.
[25] L. B. Soldano and E. C. Pennings, "Optical multi-mode interference devices based on self-imaging: Principles and applications," *J. Lightw. Technol.*, vol. 13, no. 4, pp. 615–627, Apr. 1995.
[26] "Lumerical FDTD solutions." [Online]. Available: https://www.lumerical.com